Imaging cell biology in live animals: Ready for prime time

Roberto Weigert, Natalie Porat-Shliom, and Panomwat Amornphimoltham

Intracellular Membrane Trafficking Unit, Oral and Pharyngeal Cancer Branch, National Institute of Dental and Craniofacial Research, National Institutes of Health, Bethesda, MD 20892

Time-lapse fluorescence microscopy is one of the main tools used to image subcellular structures in living cells. Yet for decades it has been applied primarily to in vitro model systems. Thanks to the most recent advancements in intravital microscopy, this approach has finally been extended to live rodents. This represents a major breakthrough that will provide unprecedented new opportunities to study mammalian cell biology in vivo and has already provided new insight in the fields of neurobiology, immunology, and cancer biology.

The discovery of GFP combined with the ability to engineer its expression in living cells has revolutionized mammalian cell biology (Chalfie et al., 1994). Since its introduction, several light microscopy–based techniques have become invaluable tools to investigate intracellular events (Lippincott-Schwartz, 2011). Among them are: time-lapse confocal microscopy, which has been instrumental in studying the dynamics of cellular and subcellular processes (Hirschberg et al., 1998; Jakobs, 2006; Cardarelli and Gratton, 2010); FRAP, which has enabled determining various biophysical properties of proteins in living cells (Berkovich et al., 2011); and fluorescence resonance energy transfer (FRET), which has been used to probe for protein–protein interactions and the local activation of specific signaling pathways (Balla, 2009). The continuous search for improvements in temporal and spatial resolution has led to the development of more sophisticated technologies, such as spinning disk microscopy, which allows the resolution of fast cellular events that occur on the order of milliseconds (Nakano, 2002); total internal reflection microscopy (TIRF), which enables imaging events in close proximity (100 nm) to the plasma membrane (Cocucci et al., 2012); and super-resolution microscopy (SIM, PALM, and STORM), which captures images with resolution higher than the diffraction limit of light (Lippincott-Schwartz, 2011).

Most of these techniques have been primarily applied to in vitro model systems, such as cells grown on solid substrates or in 3D matrices, explanted embryos, and organ cultures. These systems, which are relatively easy to maintain and to manipulate either pharmacologically or genetically, have been instrumental in providing fundamental information about cellular events down to the molecular level. However, they often fail to reconstitute the complex architecture and physiology of multicellular tissues in vivo. Indeed, in a live organism, cells exhibit a 3D organization, interact with different cell types, and are constantly exposed to a multitude of signals originated from the vasculature, the central nervous system, and the extracellular environment. For this reason, scientists have been attracted by the possibility of imaging biological processes in live multicellular organisms (i.e., intravital microscopy [IVM]). The first attempt in this direction was in 1839, when Rudolph Wagner described the interaction of leukocytes with the walls of blood vessels in the webbed feet of a live frog by using bright-field transillumination (Wagner, 1839). Since then, this approach has been used for over a century to study vascular biology in thin areas of surgically exposed organs (Irwin and MacDonald, 1953; Zweifach, 1954) or by implanting optical windows in the skin or the ears (Clark and Clark, 1932). In addition, cell migration has also been investigated using transparent tissues, such as the fin of the teleost (Wood and Thorogood, 1984; Thorogood and Wood, 1987). The introduction of epifluorescence microscopy has enabled following in more detail the dynamics of individual cells in circulation (Nuttall, 1987), in tumors (MacDonald et al., 1992), or in the immune system (von Andrian, 1996), and the spatial resolution has been significantly improved by the use of confocal microscopy, which has made it possible to collect serial optical sections from a given specimen (Villringer et al., 1989; O'Rourke and Fraser, 1990; Jester et al., 1991). However, these techniques can resolve structures only within a few micrometers from the surface of optically opaque tissues (Masedunskas et al., 2012a). It was only in the early nineteen nineties, with the development of multiphoton microscopy, that deep tissue imaging has become possible (Denk et al., 1990; Zipfel et al., 2003b), significantly contributing to several fields,

Correspondence to Roberto Weigert: weigertr@mail.nih.gov

Abbreviations used in this paper: FRET, fluorescence resonance energy transfer; IR, infrared; SHG, second harmonic generation; THG, third harmonic generation.

The Rockefeller University Press
J. Cell Biol. Vol. 201 No. 7 969–979
www.jcb.org/cgi/doi/10.1083/jcb.201212130

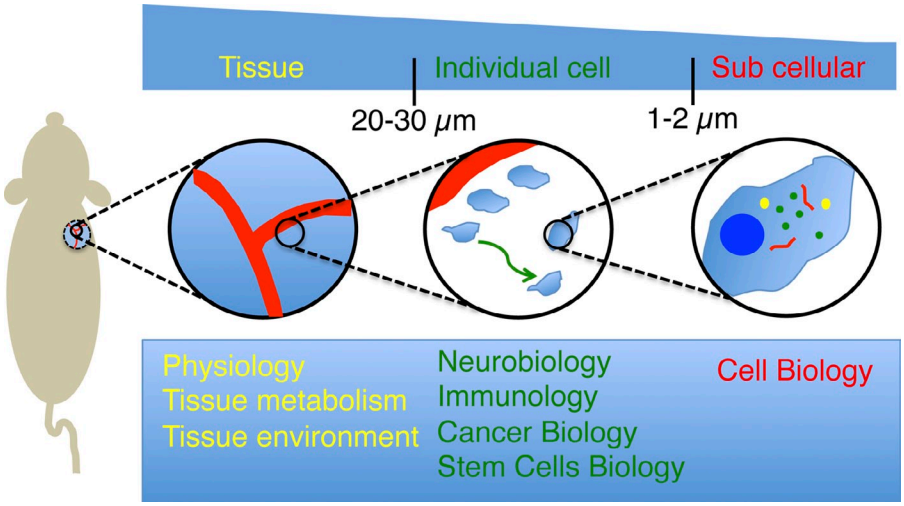

Figure 1. **Spatial resolution and current applications of intravital microscopy.** IVM provides the opportunity to image several biological processes in live animals at different levels of resolution. Low-magnification objectives (5–10×) enable visualizing tissues and their components under physiological conditions and measuring their response under pathological conditions. Particularly, the dynamics of the vasculature have been one of topic most extensively studied by IVM. Objectives with higher magnification (20–30×) have enabled imaging the behavior of individual cell over long periods of time. This has led to major breakthroughs in fields such as neurobiology, immunology, cancer biology, and stem cell research. Finally, the recent developments of strategies to minimize the motion artifacts caused by the heartbeat and respiration combined with high power lenses (60–100×) have opened the door to image subcellular structures and to study cell biology in live animals.

including neurobiology, immunology, and cancer biology (Fig. 1; Svoboda and Yasuda, 2006; Amornphimoltham et al., 2011; Beerling et al., 2011). In the last few years, the development of strategies to minimize the motion artifacts caused by the heartbeat and respiration has made it possible to successfully image subcellular structures with spatial and temporal resolutions comparable to those achieved in in vitro model systems, thus providing the opportunity to study cell biology in live mammalian tissues (Fig. 1; Weigert et al., 2010; Pittet and Weissleder, 2011).

The aim of this review is to highlight the power of IVM in addressing cell biological questions that cannot be otherwise answered in vitro, due to the intrinsic limitations of reductionist models, or by other more classical approaches. Furthermore, we discuss limitations and areas for improvement of this imaging technique, hoping to provide cell biologists with the basis to assess whether IVM is the appropriate choice to address their scientific questions.

Imaging techniques currently used to perform intravital microscopy

Confocal and two-photon microscopy are the most widely used techniques to perform IVM. Confocal microscopy, which is based on single photon excitation, is a well-established technique (Fig. 2 A) that has been extensively discussed elsewhere (Wilson, 2002); hence we will only briefly describe some of the main features of two-photon microscopy and other nonlinear optical techniques.

The first two-photon microscope (Denk et al., 1990) was based on the principle of two-photon excitation postulated by Maria Göppert-Mayer in her PhD thesis (Göppert-Mayer, 1931). In this process a fluorophore is excited by the simultaneous absorption of two photons with wavelengths in the near-infrared (IR) or IR spectrum (from 690 to 1,600 nm; Fig. 2 B). Two-photon excitation requires high-intensity light that is provided by lasers generating very short pulses (in the femtosecond range) and is focused on the excitation spot by high numerical aperture lenses (Zipfel et al., 2003b). There are three main advantages in using two-photon excitation for IVM. First, IR light has a deeper tissue penetration than UV or visible light (Theer and Denk, 2006). Indeed, two-photon microscopy can resolve structures up to a depth of 300–500 µm in most of the tissues (Fig. 2 B), and up to 1.5 mm in the brain (Theer et al., 2003; Masedunskas et al., 2012a), whereas confocal microscopy is limited to 80–100 µm (Fig. 2 A). Second, the excitation is restricted to a very small volume (1.5 fl; Fig. 2 B). This implies that in two-photon microscopy there is no need to eliminate off-focus signals, and that under the appropriate conditions photobleaching and phototoxicity are negligible (Zipfel et al., 2003b). However, confocal microscopy induces out-of-focus photodamage, and thus is less suited for long-term imaging. Third, selected endogenous molecules can be excited, thus providing the contrast to visualize specific biological structures without the need for exogenous labeling (Zipfel et al., 2003a). Some of these molecules can also be excited by confocal microscopy using UV light, although with the risk of inducing photodamage.

More recently, other nonlinear optical techniques have been used for IVM, and among them are three-photon excitation, and second and third harmonic generation (SHG and THG; Campagnola and Loew, 2003; Zipfel et al., 2003b; Oheim et al., 2006). Three-photon excitation follows the same principle as two-photon (Fig. 2 B), and can reveal endogenous molecules such as serotonin and melatonin (Zipfel et al., 2003a; Ritsma et al., 2013). In SHG and THG, photons interact with the specimen and combine to form new photons that are emitted with two or three times their initial energy (Fig. 2 C). SHG reveals collagen (Fig. 2 C) and myosin fibers (Campagnola and Loew, 2003), whereas THG reveals lipid droplets and myelin fibers (Débarre et al., 2006; Weigelin et al., 2012). Recently, two other techniques have been used for IVM: coherent anti-Stokes Raman scattering (CARS) and fluorescence lifetime imaging (FLIM). CARS that is based on two laser beams combined to match the energy gap between two vibrational levels of the molecule of interest, has been used to image lipids and myelin fibers (Müller and Zumbusch, 2007; Fu et al., 2008; Le et al., 2010). FLIM, which measures the lifetime that a molecule spends in the excited state, provides quantitative information on

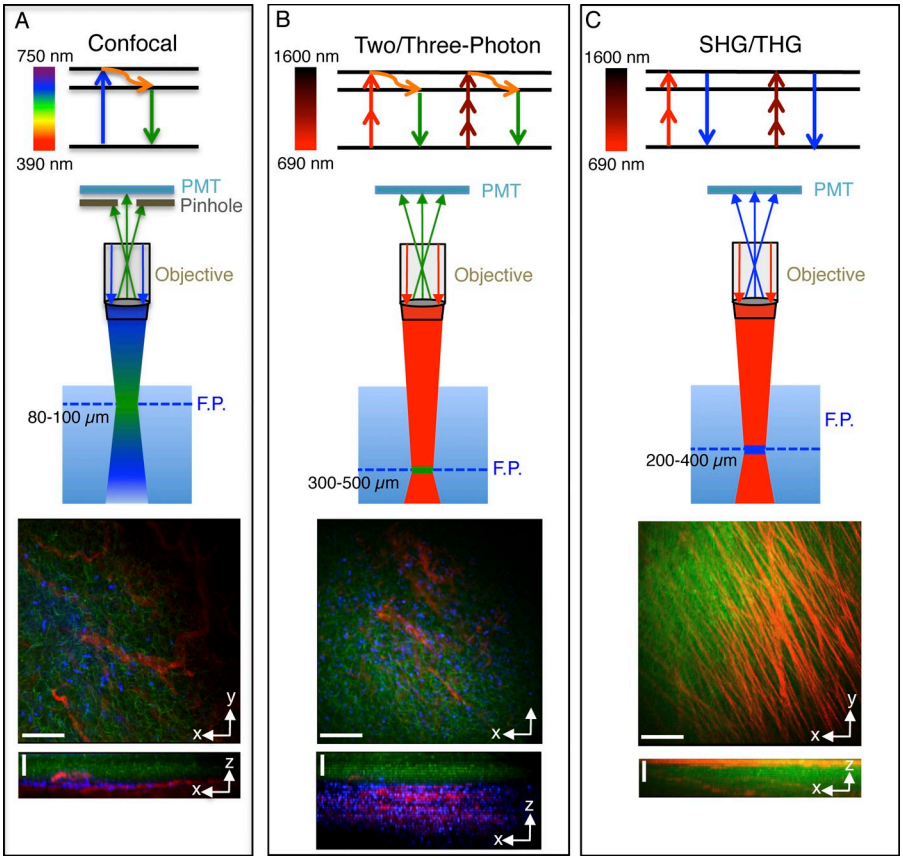

Figure 2. **Fluorescent light microscopy imaging techniques used for intravital microscopy.** (A) Confocal microscopy. (top) In confocal microscopy, a fluorophore absorbs a single photon with a wavelength in the UV-visible range of the spectrum (blue arrow). After a vibrational relaxation (orange curved arrow), a photon with a wavelength shifted toward the red is emitted (green arrow). (center) In thick tissue, excitation and emission occur in a relative large volume around the focal plane (F.P.). The off-focus emissions are eliminated through a pinhole, and the signal from the focal plane is detected via a photomultiplier (PMT). Confocal microscopy enables imaging at a maximal depth to 80–100 µm. (bottom) Confocal z stack of the tongue of a mouse expressing the membrane marker m-GFP (green) in the K14-positive basal epithelial layer, and the membrane marker mTomato in the endothelium (red). The xy view shows a maximal projection of 40 z slices acquired every 2.5 µm, whereas the xz view shows a lateral view of the stack. In blue are the nuclei labeled by a systemic injection of Hoechst. Excitation wavelengths: 450 nm, 488 nm, and 562 nm. (B) Two- and three-photon microscopy. (top) In this process a fluorophore absorbs almost simultaneously two or three photons that have half (red arrow) or a third (dark red arrow) of the energy required for its excitation with a single photon. Two- or three-photon excitations typically require near-IR or IR light (from 690 to 1,600 nm). (center) Emission and excitation occur only at the focal plane in a restricted volume (1.5 fl), and for this reason a pinhole is not required. Two- and three-photon microscopy enable imaging routinely at a maximal depth of 300–500 µm. (bottom) Two-photon z stack of an area adjacent to that imaged in A. xy view shows a maximal projection of 70 slices acquired every 5 µm. xz view shows a lateral view of the stack. Excitation wavelength: 840 nm. (C) SHG and THG. (top) In SHG and THG, photons interact with the specimen and combine to form new photons that are emitted with twice or three times their initial energy without any energy loss. (center) These processes have similar features to those described for two- and three-photon microscopy and enable imaging at a maximal depth of 200–400 µm. (bottom) z stack of a rat heart excited by two-photon microscopy (740 nm) to reveal the parenchyma (green), and SHG (930 nm) to reveal collagen fibers (red). xy shows a maximal projection of 20 slices acquired every 5 µm. xz view shows a lateral view of the stack. Bars: (xy views) 40 µm; (xz views) 50 µm.

cellular parameters such as pH, oxygen levels, ion concentration, and the metabolic state of various biomolecules (Levitt et al., 2009; Provenzano et al., 2009; Bakker et al., 2012).

We want to emphasize that two-photon microscopy and the other nonlinear techniques are the obligatory choice when the imaging area is located deep inside the tissue, endogenous molecules have to be imaged, or long-term imaging with frequent sampling is required. However, confocal microscopy is more suited to resolve structures in the micrometer range, because of the possibility of modulating the optical slice (Masedunskas et al., 2012a).

IVM to investigate biological processes at the tissue and the single cell level

The main strength of IVM is to provide information on the dynamics of biological processes that otherwise cannot be reconstituted in vitro or ex vivo. Indeed, IVM has been instrumental in studying several aspects of tissue physiopathology (Table 1). A clear example is the response of the vasculature to physiological and pathological stimuli (Fig. 3, A and B). Although other approaches such as classical immunohistochemistry, electron microscopy, and indirect immunofluorescence may provide detailed structural and quantitative information on blood vessels, IVM enables measuring events such as variations of blood flow at the level of the capillaries or local changes in blood vessel permeability. These data have been instrumental in understanding the mechanisms of ischemic diseases and tumor progression, and in designing effective anticancer treatments.

IVM has also been used successfully to study the dynamics and the morphological changes of individual cells within a tissue (Table 2). These aspects are strongly influenced by a multitude of factors that include interactions with: (1) other cell types within the tissue, (2) components of the extracellular matrix (e.g., collagen fibers), and (3) molecules coming from the vasculature (e.g., glucose, oxygen, hormones), the central and the peripheral nervous system (e.g., neurotransmitters), or the immune system (e.g., chemokines).

In neurobiology, for example, the development of approaches to perform long-term in vivo imaging has permitted the correlation of changes in neuronal morphology and neuronal circuitry to pathological conditions such as stroke (Zhang and Murphy, 2007), tumors (Barretto et al., 2011), neurodegenerative diseases (Merlini et al., 2012), and infections (McGavern and Kang, 2011). This has been accomplished by the establishment of surgical procedures to expose the brain cortex, and the implantation of chronic ports of observations such as cranial windows

Table 1. **IVM to study tissue physiopathology**

Event	Organ	Probes	Reference
Measurements of local blood flow and glial cell function	Brain	Dextran	Helmchen and Kleinfeld, 2008
Ischemia and reperfusion	Brain	Sulphorhodamine 101, Dextran	Zhang and Murphy, 2007; Masamoto et al., 2012;
Glomerular filtration and tubular reabsorption	Kidney	Dextran, Albumin	Kang et al., 2006; Yu et al., 2007; Camirand et al., 2011
Blood flow patterns	Pancreatic islets	Dextran	Nyman et al., 2008
Capillary response and synaptic activation	Olfactory bulb	Dextran	Chaigneau et al., 2003
Imaging angiogenesis during wound healing	Skullcap	Dextran	Holstein et al., 2011
Pulmonary microvasculature and endothelial activation	Lung	Dextran	Presson et al., 2011
Morphology of blood vessels and permeability in tumors	Xenografts	Dextran, RGD quantum dots	Tozer et al., 2005; Smith et al., 2008; Vakoc et al., 2009; Fukumura et al., 2010
Hepatic transport into the bile canaliculi	Liver	Carboxyfluorescein diacetate Rhodamine 123	Babbey et al., 2012; Liu et al., 2012
Progression of amyloid plaques in Alzheimer's disease	Brain	Curcumin and metoxy-04	Spires et al., 2005; Garcia-Alloza et al., 2007
Mitochondrial membrane potential	Liver	Tetramethylrhodamine methyl ester Rhodamine 123	Theruvath et al., 2008; Zhong et al., 2008
Oxygen consumption	Liver	Ru(phen3)2+	Paxian et al., 2004
Sarcomere contraction in humans	Skeletal muscle	Endogenous fluorescence	Llewellyn et al., 2008

and imaging guide tubes for micro-optical probes (Svoboda and Yasuda, 2006; Xu et al., 2007; Barretto et al., 2011). In addition, this field has thrived thanks to the development of several transgenic mouse models harboring specific neuronal populations expressing either one or multiple fluorescent molecules (Svoboda and Yasuda, 2006; Livet et al., 2007).

In tumor biology, the ability to visualize the motility of cancer cells within a tumor in vivo has provided tremendous information on the mechanisms regulating invasion and metastasis (Fig. 3 C; Beerling et al., 2011). Tumor cells metastasize to distal sites by using a combination of processes, which include tumor outgrowth, vascular intravasation, lymphatic invasion, or migration along components of the extracellular matrix and nerve fibers. Although classical histological analysis and indirect immunofluorescence have been routinely used to study these processes, the ability to perform long-term IVM through the optimization of optical windows (Alexander et al., 2008; Kedrin et al., 2008; Gligorijevic et al., 2009; Ritsma et al., 2012b) has provided unique insights. For example, a longitudinal study performed by using a combination of two-photon microscopy, SHG, and THG has highlighted the fact that various tissue components associated with melanomas may play either a migration-enhancing or migration-impeding role during collective cell invasion (Weigelin et al., 2012). In mammary tumors, the intravasation of metastatic cells has been shown to require macrophages (Wang et al., 2007; Wyckoff et al., 2007). In head and neck cancer, cells have been shown to migrate from specific sites at the edge of the tumor, and to colonize the cervical lymph nodes by migrating though the lymphatic vessels (Fig. 3 C; Amornphimoltham et al., 2013). In highly invasive melanomas, the migratory ability of cells has been correlated with their differentiation state, as determined by the expression of a reporter for melanin expression (Pinner et al., 2009).

Imaging the cells of the immune system in a live animal has revealed novel qualitative and quantitative aspects of the dynamics of cellular immunity (Fig. 2 C and Video 1; Germain et al., 2005; Cahalan and Parker, 2008; Nitschke et al., 2008). Indeed, the very complex nature of the immune response, the involvement of a multitude of tissue components, and its tight spatial and temporal coordination clearly indicate that IVM is the most suited approach to study cellular immunity. This is highlighted in studies either in lymphoid tissues, where the exquisite coordination between cell–cell interactions and cell signaling has been studied during the interactions of B lymphocytes and T cell lymphoid tissues (Qi et al., 2006), T cell activation (Hickman et al., 2008; Friedman et al., 2010), and migration of dendritic cells (Nitschké et al., 2012), or outside lymphoid tissues, such as, for example, brain during pathogen infections (Nayak et al., 2012), heart during inflammation (Li et al., 2012), and solid tumors (Deguine et al., 2010).

Imaging subcellular structures in vivo and its application to cell biology

The examples described so far convey that IVM has contributed to unraveling how the unique properties of the tissue environment in vivo significantly regulate the dynamics of individual cells and ultimately tissue physiology. Is IVM suitable to determine (1) how subcellular events occur in vivo, (2) whether they differ in in vitro settings, and (3), finally, the nature of their contribution to tissue physiology?

IVM has been extensively used to image subcellular structures in smaller organisms (i.e., zebrafish, *Caenorhabditis elegans*) that are transparent and can be easily immobilized (Rohde and Yanik, 2011; Tserevelakis et al., 2011; Hove and Craig, 2012). In addition, the ability to easily perform genetic manipulations has made these systems extremely attractive to study several aspects of developmental and cell biology. However, their differences in term of organ physiology with respect to rodents do not make them suitable models for human diseases. For a long time, subcellular imaging in live rodents has

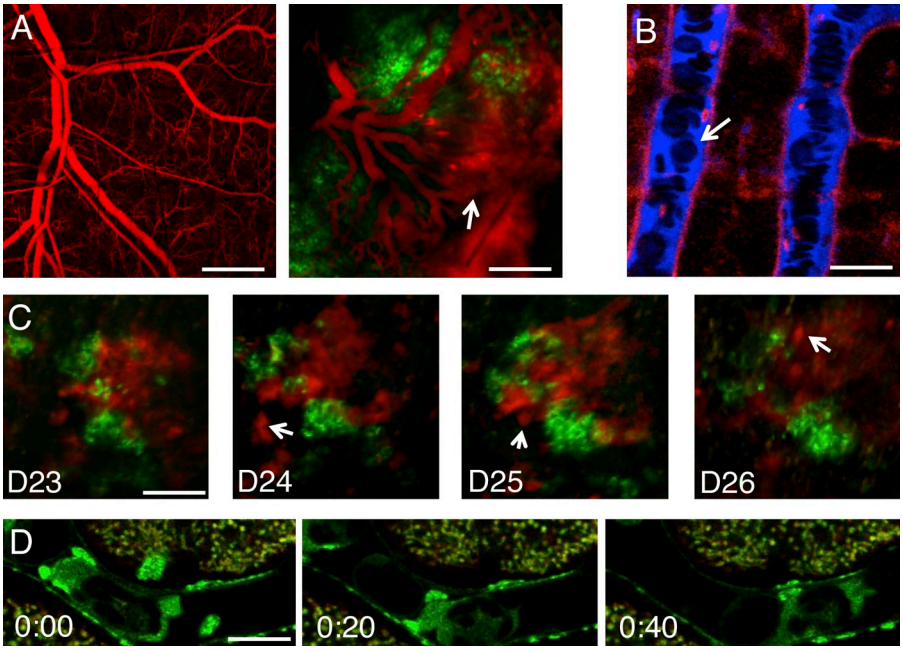

Figure 3. **Imaging tissues and individual cells in live animals.** (A) The vasculature of an immunocompromised mouse was highlighted by the systemic injection of 2 MD dextran (red) before (left) and after (right) the implant of breast cancer cells in the back (green). Note the change in shape of the blood vessels and their increased permeability (arrow). Images were acquired by two-photon microscopy (excitation wavelength: 930 nm). (B) The microvasculature in the liver of a mouse expressing the membrane marker mTomato (red) was highlighted by the injection of cascade blue dextran (blue) and imaged by confocal microscopy (excitation wavelengths: 405 nm and 561 nm). Note the red blood cells that do not uptake the dye and appear as dark objects in the blood stream (arrow). (C) Metastatic and nonmetastatic human adenocarcinoma cells were injected in the tongue of an immunocompromised mouse and imaged for four consecutive days by using two-photon microscopy (excitation wavelength: 930 nm). The metastatic cells, which express the fluorescent protein mCherry (red), migrate away from the edge of the tumor (arrows), whereas the nonmetastatic cells, which express the fluorescent protein Venus (green), do not. (D) A granulocyte moving inside a blood vessel in the mammary gland of a mouse expressing GFP-tagged myosin IIb (green) and labeled with the mitochondrial vital dye MitoTracker (red) was imaged in time lapse by using confocal microscopy (excitation wavelengths: 488 nm and 561 nm). Figure corresponds to Video 1. Time is expressed as minutes:seconds. Bars: (A) 100 µm; (B) 10 µm; (C) 30 µm; (D) 10 µm.

been hampered by the motion artifacts derived from the heartbeat and respiration. Indeed, small shifts along the three axes make it practically impossible to visualize structures whose sizes are in the micrometer or submicrometer range, whereas it marginally affects larger structures. This issue has been only recently addressed by using a combination of strategies, which include: (1) the development of specific surgical procedures that allow the exposure and proper positioning of the organ of interest (Masedunskas et al., 2013), (2) the improvement of specific organ holders (Cao et al., 2012; Masedunskas et al., 2012a), and (3) the synchronization of the imaging acquisition with the heartbeat and respiration (Presson et al., 2011; Li et al., 2012). Very importantly, these approaches have been successfully implemented without compromising the integrity and the physiology of the tissue, thus opening the door to study cell biology in a live animal.

For example, large subcellular structures such as the nuclei have been easily imaged, making it possible to study processes such as cell division and apoptosis (Fig. 4 A; Goetz et al., 2011; Orth et al., 2011; Rompolas et al., 2012). Interestingly, these studies have highlighted the fact that the in vivo microenvironment substantially affects nuclear dynamics. Indeed, mitosis and the structure of the mitotic spindle were followed over time in a xenograft model of human cancer expressing the histone marker mCherry-H2B and GFP-tubulin (Orth et al., 2011). Specifically, the effects of the anticancer drug Paclitaxel were studied, revealing that the tumor cells in vivo have a higher mitotic index and lower pro-apoptotic propensity than in vitro (Orth et al., 2011). FRET has been used in subcutaneous tumors to image cytotoxic T lymphocyte–induced apoptosis and highlighted that the kinetics of this process are much slower than those reported for nontumor cells in vivo that are exposed to a different microenvironment (Breart et al., 2008). Cell division has also been followed in the hair-follicle stem cells of transgenic mice expressing GFP-H2B. This study determined that epithelial–mesenchymal interactions are essential for stem cell activation and regeneration, and that nuclear divisions occur in a specific area of the hair follicles and are oriented toward the axis of growth (Rompolas et al., 2012). These processes show an extremely high level of temporal and spatial organization that can only be appreciated in vivo and by using time-lapse imaging.

Imaging membrane trafficking has been more challenging because of its dynamic nature and the size of the structures to image. The first successful attempt to visualize membrane traffic events was achieved in the kidney of live rats by using two-photon microscopy where the endocytosis of fluid-phase markers, such as dextrans, or the receptor-mediated uptake of folate, albumin, and the aminoglycoside gentamicin were followed in the proximal tubuli (Fig. 4 D and Video 2; Dunn et al., 2002; Sandoval et al., 2004; Russo et al., 2007). These pioneering studies showed for the first time that apical uptake is involved in the filtration of large molecules in the kidney, whereas previously it was believed to be exclusively due to a barrier in the glomerular capillary wall. However, in the kidney the residual motion artifacts limited the imaging to short periods of time. Recently, the salivary glands have proven to be a suitable organ to study the dynamics of membrane trafficking by using either two-photon or confocal microscopy. Systemically injected dextrans, BSA, and transferrin were observed to rapidly internalize in the stromal cells surrounding the salivary gland epithelium in a process dependent on the actin cytoskeleton (Masedunskas and Weigert, 2008; Masedunskas et al., 2012b). Moreover, the trafficking of these molecules through the endo-lysosomal system was documented, providing interesting insights on early endosomal

Table 2. **IVM to study the dynamics of individual cells**

Event	Organ	Probe	Reference
Neuronal morphology of hippocampal neurons	Brain	Thy1-GFP mice, dextran	Barretto et al., 2011
Neuronal circuitry	Brain	Brainbow mice	Livet et al., 2007
Dendritic spine development in the cortex	Brain	YFP H-line mice	Pan and Gan, 2008
Calcium imaging in the brain	Brain	GCAMP	Zariwala et al., 2012
Natural killer cell and cytotoxic T cell interactions with tumors	Xenograft	mCFP , mYFP	Deguine et al., 2010
Neutrophil recruitment in beating heart	Heart	Dextran, CX3CR1-GFP mice	Li et al., 2012
Immune cells in the central nervous system	Brain	Dextran, CX3CR1-GFP, LysM-GFP and CD11c-YFP mice	Nayak et al., 2012
Dendritic cells migration	Skin	YFP, VE-caherin RFP mice, dextran	Nitschké et al., 2012
CD8+ T cells interaction with dendritic cells during viral infection	Lymph nodes	EGFP, Dextran, SHG	Hickman et al., 2008
B cells and dendritic cells interactions outside lymph nodes	Lymph nodes	EGFP	Qi et al., 2006
Change in gene expression during metastasis	Xenograft		Pinner et al., 2009
Invasion and metastasis in head and neck cancer	Xenograft	YFP, RFP-lifeact, dextran	Amornphimoltham et al., 2013
Fibrosarcoma cell migration along collagen fibers	Dorsal skin chamber	SHG, EGFP, DsRed, Dextran	Alexander et al., 2008
Long term imaging mammary tumors and photo-switchable probes	Mammary window	Dendra-2	Kedrin et al., 2008; Gligorijevic et al., 2009
Long term imaging liver metastasis through abdominal window	Liver	SHG, Dendra2, EGFP	Ritsma et al., 2012b
Macrophages during intravasation in mammary tumors	Xenograft	EGFP, SHG, dextrans	Wang et al., 2007; Wyckoff et al., 2007
Melanoma collective migration	Dorsal skin Chamber	SHG, THG, EGFP, Dextran	Weigelin et al., 2012
Hematopoietic stem cells and blood vessel	Skullcup	Dextran	Lo Celso et al., 2009
Epithelial stem cells during hair regeneration	Skin	H2B-GFP mice	Rompolas et al., 2012

fusion (Fig. 4 E; Masedunskas and Weigert, 2008; Masedunskas et al., 2012b). Notably, significant differences were observed in the kinetics of internalization of transferrin and dextran. In vivo, dextran was rapidly internalized by stromal cells, whereas transferrin appeared in endosomal structures after 10–15 min. However, in freshly explanted stromal cells adherent on glass, transferrin was internalized within 1 min, whereas dextran appeared in endosomal structures after 10–15 min. Although the reasons for this difference were not addressed, it is clear that the environment in vivo has profound effects on the regulation of intracellular processes (Masedunskas et al., 2012b). Similar differences have been reported for the caveolae that in vivo are more dynamic than in cell cultures (Thomsen et al., 2002; Oh et al., 2007). Endocytosis has also been investigated in the epithelium of the salivary glands (Sramkova et al., 2009). Specifically, plasmid DNA was shown to be internalized by a clathrin-independent pathway from the apical plasma membrane of acinar and ductal cells, and to subsequently escape from the endo-lysosomal system, thus providing useful information on the mechanisms of nonviral gene delivery in vivo (Sramkova et al., 2012). Receptor-mediated endocytosis has also been studied in cancer models. Indeed, the uptake of a fluorescent EGF conjugated to carbon nanotubes has been followed in xenografts of head and neck cancer cells revealing that the internalization occurs primarily in cells that express high levels of EGFR (Bhirde et al., 2009). The role of endosomal recycling has also been investigated during tumor progression. Indeed, the small GTPase Rab25 was found to regulate the ability of head neck cancer cells to migrate to lymph nodes by controlling the dynamic assembly of plasma membrane actin reach protrusion in vivo (Amornphimoltham et al., 2013). Interestingly, this activity of Rab25 was reconstituted in cells migrating through a 3D collagen matrix but not in cells grown adherent to a solid substrate.

IVM has been a powerful tool in investigating the molecular machinery controlling regulated exocytosis in various organs. In salivary glands, the use of selected transgenic mice expressing either soluble GFP or a membrane-targeted peptide has permitted the characterization of the dynamics of exocytosis of the secretory granules after fusion with the plasma membrane (Fig. 4 E; Masedunskas et al., 2011a, 2012d). These studies revealed that the regulation and the modality of exocytosis differ between in vivo and in vitro systems. Indeed, in vivo, regulated exocytosis is controlled by stimulation of the β-adrenergic receptor, and secretory granules undergo a gradual collapse after fusion with the apical plasma membrane, whereas, in vitro, regulated exocytosis is also controlled by the muscarinic receptor and the secretory granules fuse to each other, forming strings of interconnected vesicles at the plasma membrane (compound exocytosis; Masedunskas et al., 2011a, 2012d). Moreover, the transient expression of reporter molecules for F-actin has revealed the requirement for the assembly of an actomyosin complex to facilitate the completion of the exocytic process (Masedunskas et al., 2011a, 2012d). This result underscores the fact that the dynamics of the assembly of the actin cytoskeleton can be studied both qualitatively and quantitatively in live animals at the level of individual secretory granules. In addition, this approach has highlighted some of the mechanisms that contribute to regulate the apical plasma membrane homeostasis in vivo that cannot be recapitulated in an in vitro model systems (Masedunskas et al., 2011b, 2012c; Porat-Shliom et al., 2013). Indeed, the hydrostatic pressure that is built inside the ductal system by the secretion of fluids that accompanies exocytosis plays a significant role in controlling the

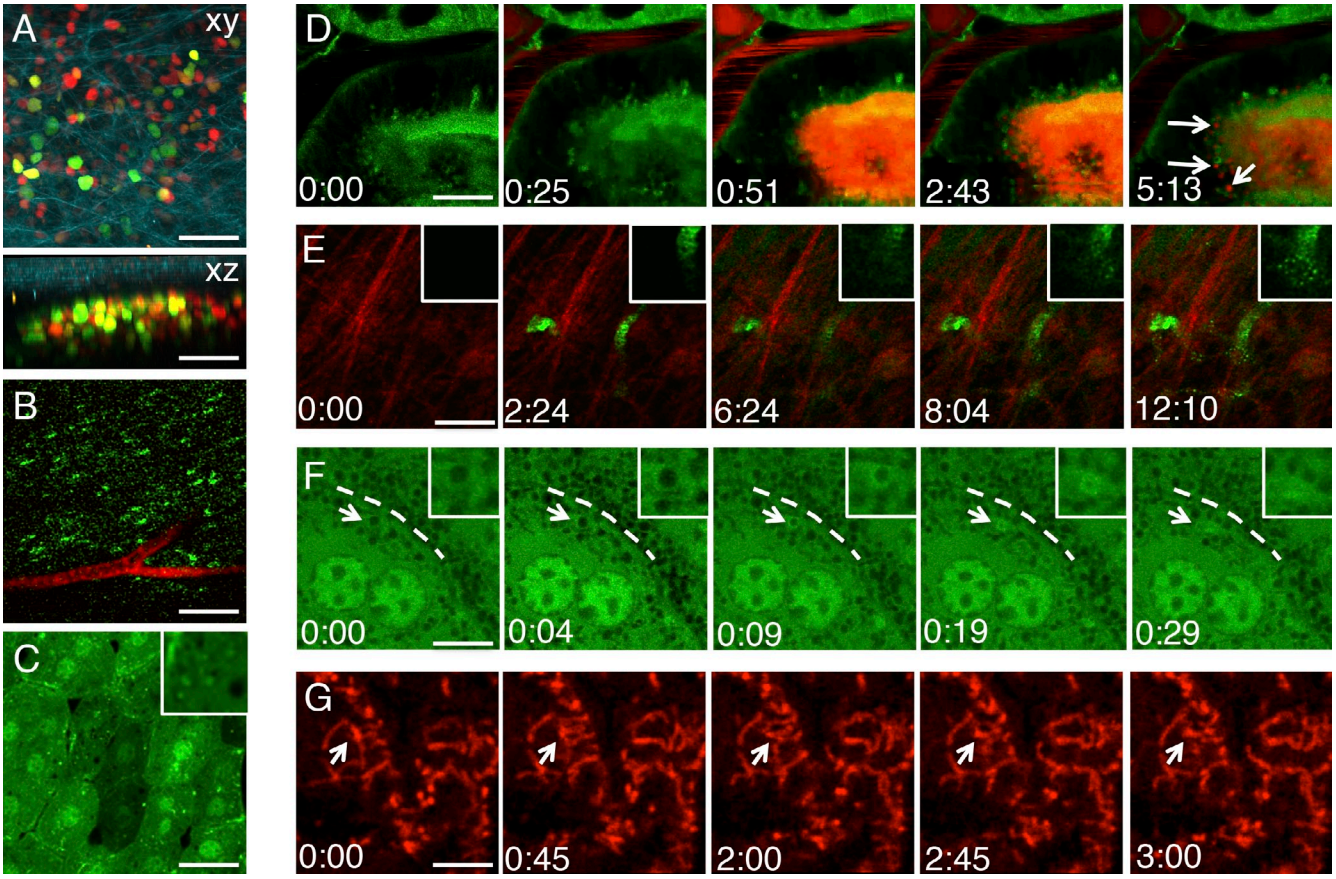

Figure 4. **Imaging subcellular events in live animals.** (A) Human squamous carcinoma cells were engineered to stably express the Fucci cell cycle reporter into the nucleus and injected in the back of an immunocompromised mouse. After 1 wk, the tumor was imaged by two-photon microscopy and SHG (excitation wavelength: 930 nm). (top) Maximal projection of a z stack (xy view). Cells in G2/M are in green, cells in G1 are in red, and collagen fibers are in cyan. (bottom) Lateral view (xz) of a z stack. (B) Clusters of GLUT4-containing vesicles (green) in the soleus muscle of a transgenic mouse expressing GFP-GLUT4 and injected with 70 kD Texas red–dextran to visualize the vasculature and imaged by two-photon microscopy (excitation wavelength: 930 nm). (C) Confocal microscopy (excitation wavelength: 488 nm) of hepatocytes in the liver of a transgenic mouse expressing the autophagy marker GFP-LC3. The inset shows small GFP-LC3 autophagic vesicles. (D–G) Dynamics of intracellular compartments imaged by time-lapse two-photon (E) or confocal microscopy (D, F, and G). (D) Endocytosis of systemically injected 10 kD Texas red–dextran into the kidney of a transgenic mouse expressing the membrane marker m-GFP. The dextran (red) is transported from the microvasculature into the proximal tubuli, and then internalized in small endocytic vesicles (arrows; Video 2). (E) Endocytosis of a systemically injected 10 kD of Alexa Fluor 488 dextran into the salivary glands of a live rat. The dextran (green) diffuses from the vasculature into the stroma, and it is internalized by stromal cells (insets). Collagen fibers (red) are highlighted by SHG. (F) Regulated exocytosis of large secretory granules in the salivary glands of a live transgenic mouse expressing cytoplasmic GFP. The GFP is excluded from the secretory granules and accumulates on their limiting membranes (arrows) after fusion with the plasma membrane (broken lines). The gradual collapse of an individual granule is highlighted in the insets. (G) Dynamics of mitochondria labeled with the membrane potential dye TMRM in the salivary glands of a live mouse. Time is expressed as minutes:seconds. Bars: (A) 40 µm; (B) 15 µm; (C, D, E, and G) 10 µm; (F) 5 µm.

dynamics of secretory granules at the apical plasma membrane. This aspect has never been appreciated in organ explants where the integrity of the ductal system is compromised. Finally, a very promising model has been developed in the skeletal muscle, where the transient transfection of a GFP-tagged version of the glucose transporter type 4 (GLUT4) has made possible to characterize the kinetics of the GLUT4-containing vesicles in resting conditions and their insulin-dependent translocation to the plasma membrane (Fig. 4 B; Lauritzen et al., 2008, 2010). This represents a very powerful experimental model that bridges together physiology and cell biology and has the potential to provide fundamental information on metabolic diseases.

These examples underscore the merits of subcellular IVM to investigate specific areas of cell biology such as membrane trafficking, the cell cycle, apoptosis, and cytoskeletal organization. However, IVM is rapidly extending to other areas, such as cell signaling (Stockholm et al., 2005; Rudolf et al., 2006; Ritsma et al., 2012a), metabolism (Fig. 4 C; Débarre et al., 2006; Cao et al., 2012), mitochondrial dynamics (Fig. 4 F; Sun et al., 2005; Hall et al., 2013), or gene and protein expression (Pinner et al., 2009) that have just begun to be explored.

Future perspectives

IVM has become a powerful tool to study biological processes in live animals that is destined to have an enormous impact on cell biology. The examples described here give a clear picture of the broad applicability of this approach. In essence, we foresee that IVM is going to be the obligatory choice to study highly dynamic subcellular processes that cannot be reconstituted in vitro or ex vivo, or when a link between cellular events and tissue physiopathology is being pursued. In addition, IVM will provide the opportunity to complement and confirm data

generated from in vitro studies. Importantly, the fact that in several instances confocal microscopy can be effectively used for subcellular IVM makes this approach immediately accessible to several investigators.

In terms of future directions, we envision that other light microscopy techniques will soon become standard tools for in vivo studies, as shown by the recent application of FRET to study signaling (Stockholm et al., 2005; Rudolf et al., 2006; Breart et al., 2008; Ritsma et al., 2012a), and FRAP, which has been used in the live brain to measure the diffusion of α synuclein, thus opening the door to studying the biophysical properties of proteins in vivo (Unni et al., 2010). Moreover, super-resolution microscopy may be applied for imaging live animals, although this task may pose some challenges. Indeed, these techniques require: (1) the complete stability of the specimen, (2) extended periods of time for light collection, (3) substantial modifications to the existing microscopes, and (4) the generation of transgenic mice expressing photoactivatable probes.

To reach its full potential, IVM has to further develop two main aspects: animal models and instrumentations. Indeed, a significant effort has to be invested in developing novel transgenic mouse models, which express fluorescently labeled reporter molecules. One example is the recently developed mouse that expresses fluorescently tagged lifeact. This model will provide the unique opportunity to study F-actin dynamics in vivo in the context of processes such as cell migration and membrane trafficking (Riedl et al., 2010). Moreover, the possibility of crossing these reporter mice with knockout animals will provide the means to further study cellular processes at a molecular level. Alternatively, reporter molecules or other transgenes that may perturb a specific cellular pathway can be transiently transfected into live animals in several ways. Indeed, the remarkable advancements in gene therapy have contributed to the development of several nonviral- and viral-mediated strategies for gene delivery to selected target organs. In this respect, the salivary glands and the skeletal muscle are two formidable model systems because either transgenes or siRNAs can be successfully delivered without any adverse reaction and expressed in a few hours. In terms of the current technical limitations of IVM, the main areas of improvement are the temporal resolution, the ability to access the organ of interest with minimal invasion, and the ability to perform long-term imaging. As for the temporal resolution, the issue has begun to be addressed by using two different approaches: (1) the use of spinning disk microscopy, as shown by its recent application to image platelet dynamics in live mice (Jenne et al., 2011); and (2) the development of confocal and two-photon microscopes equipped with resonant scanners that permit increasing the scanning speed to 30 frames per second (Kirkpatrick et al., 2012). As for accessing the organs, recently several microlenses (350 µm in diameter) have been inserted or permanently implanted into live animals, minimizing the exposure of the organs and the risk of affecting their physiology (Llewellyn et al., 2008). Finally, although some approaches for the long-term imaging of the brain, the mammary glands, and the liver have been developed, additional effort has to be devoted to establish chronic ports of observations in other organs.

In conclusion, these are truly exciting times, and a new era full of novel discoveries is just around the corner. The ability to see processes inside the cells of a live animal is no longer a dream.

Online supplemental material

Video 1 shows time-lapse confocal microscopy of a granulocyte moving inside a blood vessel in the mammary gland of a mouse expressing GFP-tagged myosin IIb (green) and labeled with MitoTracker (red). Video 2 shows time-lapse confocal microscopy of the endocytosis of systemically injected 10 kD Texas red–dextran (red) into the kidney-proximal tubuli of a transgenic mouse expressing the membrane marker m-GFP (green). Online supplemental material is available at http://www.jcb.org/cgi/content/full/jcb.201212130/DC1.

This research was supported by the Intramural Research Program of the National Institutes of Health, National Institute of Dental and Craniofacial Research.

Submitted: 24 December 2012
Accepted: 30 May 2013

References

Alexander, S., G.E. Koehl, M. Hirschberg, E.K. Geissler, and P. Friedl. 2008. Dynamic imaging of cancer growth and invasion: a modified skin-fold chamber model. *Histochem. Cell Biol.* 130:1147–1154. http://dx.doi.org/10.1007/s00418-008-0529-1

Amornphimoltham, P., A. Masedunskas, and R. Weigert. 2011. Intravital microscopy as a tool to study drug delivery in preclinical studies. *Adv. Drug Deliv. Rev.* 63:119–128. http://dx.doi.org/10.1016/j.addr.2010.09.009

Amornphimoltham, P., K. Rechache, J. Thompson, A. Masedunskas, K. Leelahavanichkul, V. Patel, A. Molinolo, J.S. Gutkind, and R. Weigert. 2013. Rab25 regulates invasion and metastasis in head and neck cancer. *Clin. Cancer Res.* 19:1375–1388. http://dx.doi.org/10.1158/1078-0432.CCR-12-2858

Babbey, C.M., J.C. Ryan, E.M. Gill, M.S. Ghabril, C.R. Burch, A. Paulman, and K.W. Dunn. 2012. Quantitative intravital microscopy of hepatic transport. *IntraVital*. 1:44–53. http://dx.doi.org/10.4161/intv.21296

Bakker, G.J., V. Andresen, R.M. Hoffman, and P. Friedl. 2012. Fluorescence lifetime microscopy of tumor cell invasion, drug delivery, and cytotoxicity. *Methods Enzymol.* 504:109–125. http://dx.doi.org/10.1016/B978-0-12-391857-4.00005-7

Balla, T. 2009. Green light to illuminate signal transduction events. *Trends Cell Biol.* 19:575–586. http://dx.doi.org/10.1016/j.tcb.2009.08.001

Barretto, R.P., T.H. Ko, J.C. Jung, T.J. Wang, G. Capps, A.C. Waters, Y. Ziv, A. Attardo, L. Recht, and M.J. Schnitzer. 2011. Time-lapse imaging of disease progression in deep brain areas using fluorescence microendoscopy. *Nat. Med.* 17:223–228. http://dx.doi.org/10.1038/nm.2292

Beerling, E., L. Ritsma, N. Vrisekoop, P.W. Derksen, and J. van Rheenen. 2011. Intravital microscopy: new insights into metastasis of tumors. *J. Cell Sci.* 124:299–310. http://dx.doi.org/10.1242/jcs.072728

Berkovich, R., H. Wolfenson, S. Eisenberg, M. Ehrlich, M. Weiss, J. Klafter, Y.I. Henis, and M. Urbakh. 2011. Accurate quantification of diffusion and binding kinetics of non-integral membrane proteins by FRAP. *Traffic*. 12:1648–1657. http://dx.doi.org/10.1111/j.1600-0854.2011.01264.x

Bhirde, A.A., V. Patel, J. Gavard, G. Zhang, A.A. Sousa, A. Masedunskas, R.D. Leapman, R. Weigert, J.S. Gutkind, and J.F. Rusling. 2009. Targeted killing of cancer cells in vivo and in vitro with EGF-directed carbon nanotube-based drug delivery. *ACS Nano*. 3:307–316. http://dx.doi.org/10.1021/nn800551s

Breart, B., F. Lemaître, S. Celli, and P. Bousso. 2008. Two-photon imaging of intratumoral CD8+ T cell cytotoxic activity during adoptive T cell therapy in mice. *J. Clin. Invest.* 118:1390–1397. http://dx.doi.org/10.1172/JCI34388

Cahalan, M.D., and I. Parker. 2008. Choreography of cell motility and interaction dynamics imaged by two-photon microscopy in lymphoid organs. *Annu. Rev. Immunol.* 26:585–626. http://dx.doi.org/10.1146/annurev.immunol.24.021605.090620

Camirand, G., Q. Li, A.J. Demetris, S.C. Watkins, W.D. Shlomchik, D.M. Rothstein, and F.G. Lakkis. 2011. Multiphoton intravital microscopy of the transplanted mouse kidney. *Am. J. Transplant.* 11:2067–2074. http://dx.doi.org/10.1111/j.1600-6143.2011.03671.x

Campagnola, P.J., and L.M. Loew. 2003. Second-harmonic imaging microscopy for visualizing biomolecular arrays in cells, tissues and organisms. *Nat. Biotechnol.* 21:1356–1360. http://dx.doi.org/10.1038/nbt894

Cao, L., S. Kobayakawa, A. Yoshiki, and K. Abe. 2012. High resolution intravital imaging of subcellular structures of mouse abdominal organs using a microstage device. *PLoS ONE*. 7:e33876. http://dx.doi.org/10.1371/journal.pone.0033876

Cardarelli, F., and E. Gratton. 2010. In vivo imaging of single-molecule translocation through nuclear pore complexes by pair correlation functions. *PLoS ONE*. 5:e10475. http://dx.doi.org/10.1371/journal.pone.0010475

Chaigneau, E., M. Oheim, E. Audinat, and S. Charpak. 2003. Two-photon imaging of capillary blood flow in olfactory bulb glomeruli. *Proc. Natl. Acad. Sci. USA*. 100:13081–13086. http://dx.doi.org/10.1073/pnas.2133652100

Chalfie, M., Y. Tu, G. Euskirchen, W.W. Ward, and D.C. Prasher. 1994. Green fluorescent protein as a marker for gene expression. *Science*. 263:802–805. http://dx.doi.org/10.1126/science.8303295

Clark, E.R., and E.L. Clark. 1932. Observations on living preformed vessels as seen in the transparent chamber inserted into a rabbit's ear. *Am. J. Anat.* 49:441–477. http://dx.doi.org/10.1002/aja.1000490306

Cocucci, E., F. Aguet, S. Boulant, and T. Kirchhausen. 2012. The first five seconds in the life of a clathrin-coated pit. *Cell*. 150:495–507. http://dx.doi.org/10.1016/j.cell.2012.05.047

Débarre, D., W. Supatto, A.M. Pena, A. Fabre, T. Tordjmann, L. Combettes, M.C. Schanne-Klein, and E. Beaurepaire. 2006. Imaging lipid bodies in cells and tissues using third-harmonic generation microscopy. *Nat. Methods*. 3:47–53. http://dx.doi.org/10.1038/nmeth813

Deguine, J., B. Breart, F. Lemaître, J.P. Di Santo, and P. Bousso. 2010. Intravital imaging reveals distinct dynamics for natural killer and CD8(+) T cells during tumor regression. *Immunity*. 33:632–644. http://dx.doi.org/10.1016/j.immuni.2010.09.016

Denk, W., J.H. Strickler, and W.W. Webb. 1990. Two-photon laser scanning fluorescence microscopy. *Science*. 248:73–76. http://dx.doi.org/10.1126/science.2321027

Dunn, K.W., R.M. Sandoval, K.J. Kelly, P.C. Dagher, G.A. Tanner, S.J. Atkinson, R.L. Bacallao, and B.A. Molitoris. 2002. Functional studies of the kidney of living animals using multicolor two-photon microscopy. *Am. J. Physiol. Cell Physiol.* 283:C905–C916. http://dx.doi.org/10.1152/ajpcell.00159.2002

Friedman, R.S., P. Beemiller, C.M. Sorensen, J. Jacobelli, and M.F. Krummel. 2010. Real-time analysis of T cell receptors in naive cells in vitro and in vivo reveals flexibility in synapse and signaling dynamics. *J. Exp. Med.* 207:2733–2749. http://dx.doi.org/10.1084/jem.20091201

Fu, Y., T.B. Huff, H.W. Wang, H. Wang, and J.X. Cheng. 2008. Ex vivo and in vivo imaging of myelin fibers in mouse brain by coherent anti-Stokes Raman scattering microscopy. *Opt. Express*. 16:19396–19409. http://dx.doi.org/10.1364/OE.16.019396

Fukumura, D., D.G. Duda, L.L. Munn, and R.K. Jain. 2010. Tumor microvasculature and microenvironment: novel insights through intravital imaging in pre-clinical models. *Microcirculation*. 17:206–225. http://dx.doi.org/10.1111/j.1549-8719.2010.00029.x

Garcia-Alloza, M., L.A. Borrelli, A. Rozkalne, B.T. Hyman, and B.J. Bacskai. 2007. Curcumin labels amyloid pathology in vivo, disrupts existing plaques, and partially restores distorted neurites in an Alzheimer mouse model. *J. Neurochem.* 102:1095–1104. http://dx.doi.org/10.1111/j.1471-4159.2007.04613.x

Germain, R.N., F. Castellino, M. Chieppa, J.G. Egen, A.Y. Huang, L.Y. Koo, and H. Qi. 2005. An extended vision for dynamic high-resolution intravital immune imaging. *Semin. Immunol.* 17:431–441. http://dx.doi.org/10.1016/j.smim.2005.09.003

Gligorijevic, B., D. Kedrin, J.E. Segall, J. Condeelis, and J. van Rheenen. 2009. Dendra2 photoswitching through the Mammary Imaging Window. *J. Vis. Exp.* pii:1278.

Goetz, M., J.V. Ansems, P.R. Galle, M. Schuchmann, and R. Kiesslich. 2011. In vivo real-time imaging of the liver with confocal endomicroscopy permits visualization of the temporospatial patterns of hepatocyte apoptosis. *Am. J. Physiol. Gastrointest. Liver Physiol.* 301:G764–G772. http://dx.doi.org/10.1152/ajpgi.00175.2011

Göppert-Mayer, M. 1931. Uber elementarakte mit zwei quantensprungen. *Ann. Phys*. 401:273–294. http://dx.doi.org/10.1002/andp.19314010303

Hall, A.M., G.J. Rhodes, R.M. Sandoval, P.R. Corridon, and B.A. Molitoris. 2013. In vivo multiphoton imaging of mitochondrial structure and function during acute kidney injury. *Kidney Int.* 83:72–83. http://dx.doi.org/10.1038/ki.2012.328

Helmchen, F., and D. Kleinfeld. 2008. Chapter 10. In vivo measurements of blood flow and glial cell function with two-photon laser-scanning microscopy. *Methods Enzymol.* 444:231–254. http://dx.doi.org/10.1016/S0076-6879(08)02810-3

Hickman, H.D., K. Takeda, C.N. Skon, F.R. Murray, S.E. Hensley, J. Loomis, G.N. Barber, J.R. Bennink, and J.W. Yewdell. 2008. Direct priming of antiviral CD8+ T cells in the peripheral interfollicular region of lymph nodes. *Nat. Immunol.* 9:155–165. http://dx.doi.org/10.1038/ni1557

Hirschberg, K., C.M. Miller, J. Ellenberg, J.F. Presley, E.D. Siggia, R.D. Phair, and J. Lippincott-Schwartz. 1998. Kinetic analysis of secretory protein traffic and characterization of golgi to plasma membrane transport intermediates in living cells. *J. Cell Biol.* 143:1485–1503. http://dx.doi.org/10.1083/jcb.143.6.1485

Holstein, J.H., S.C. Becker, M. Fiedler, P. Garcia, T. Histing, M. Klein, M.W. Laschke, M. Corsten, T. Pohlemann, and M.D. Menger. 2011. Intravital microscopic studies of angiogenesis during bone defect healing in mice calvaria. *Injury*. 42:765–771. http://dx.doi.org/10.1016/j.injury.2010.11.020

Hove, J.R., and M.P. Craig. 2012. High-speed confocal imaging of zebrafish heart development. *Methods Mol. Biol.* 843:309–328. http://dx.doi.org/10.1007/978-1-61779-523-7_26

Irwin, J.W., and J. MacDonald III. 1953. Microscopic observations of the intrahepatic circulation of living guinea pigs. *Anat. Rec.* 117:1–15. http://dx.doi.org/10.1002/ar.1091170102

Jakobs, S. 2006. High resolution imaging of live mitochondria. *Biochim. Biophys. Acta*. 1763:561–575. http://dx.doi.org/10.1016/j.bbamcr.2006.04.004

Jenne, C.N., C.H. Wong, B. Petri, and P. Kubes. 2011. The use of spinning-disk confocal microscopy for the intravital analysis of platelet dynamics in response to systemic and local inflammation. *PLoS ONE*. 6:e25109. http://dx.doi.org/10.1371/journal.pone.0025109

Jester, J.V., P.M. Andrews, W.M. Petroll, M.A. Lemp, and H.D. Cavanagh. 1991. In vivo, real-time confocal imaging. *J. Electron Microsc. Tech.* 18:50–60. http://dx.doi.org/10.1002/jemt.1060180108

Kang, J.J., I. Toma, A. Sipos, F. McCulloch, and J. Peti-Peterdi. 2006. Quantitative imaging of basic functions in renal (patho)physiology. *Am. J. Physiol. Renal Physiol.* 291:F495–F502. http://dx.doi.org/10.1152/ajprenal.00521.2005

Kedrin, D., B. Gligorijevic, J. Wyckoff, V.V. Verkhusha, J. Condeelis, J.E. Segall, and J. van Rheenen. 2008. Intravital imaging of metastatic behavior through a mammary imaging window. *Nat. Methods*. 5:1019–1021. http://dx.doi.org/10.1038/nmeth.1269

Kirkpatrick, N.D., E. Chung, D.C. Cook, X. Han, G. Gruionu, S. Liao, L.L. Munn, T.P. Padera, D. Fukumura, and R.K. Jain. 2012. Video-rate resonant scanning multiphoton microscopy: An emerging technique for intravital imaging of the tumor microenvironment. *IntraVital*. 1:60–68. http://dx.doi.org/10.4161/intv.21557

Lauritzen, H.P., H. Galbo, J. Brandauer, L.J. Goodyear, and T. Ploug. 2008. Large GLUT4 vesicles are stationary while locally and reversibly depleted during transient insulin stimulation of skeletal muscle of living mice: imaging analysis of GLUT4-enhanced green fluorescent protein vesicle dynamics. *Diabetes*. 57:315–324. http://dx.doi.org/10.2337/db06-1578

Lauritzen, H.P., H. Galbo, T. Toyoda, and L.J. Goodyear. 2010. Kinetics of contraction-induced GLUT4 translocation in skeletal muscle fibers from living mice. *Diabetes*. 59:2134–2144. http://dx.doi.org/10.2337/db10-0233

Le, T.T., S. Yue, and J.X. Cheng. 2010. Shedding new light on lipid biology with coherent anti-Stokes Raman scattering microscopy. *J. Lipid Res.* 51:3091–3102. http://dx.doi.org/10.1194/jlr.R008730

Levitt, J.A., D.R. Matthews, S.M. Ameer-Beg, and K. Suhling. 2009. Fluorescence lifetime and polarization-resolved imaging in cell biology. *Curr. Opin. Biotechnol.* 20:28–36. http://dx.doi.org/10.1016/j.copbio.2009.01.004

Li, W., R.G. Nava, A.C. Bribriesco, B.H. Zinselmeyer, J.H. Spahn, A.E. Gelman, A.S. Krupnick, M.J. Miller, and D. Kreisel. 2012. Intravital 2-photon imaging of leukocyte trafficking in beating heart. *J. Clin. Invest.* 122:2499–2508. http://dx.doi.org/10.1172/JCI62970

Lippincott-Schwartz, J. 2011. Emerging in vivo analyses of cell function using fluorescence imaging (*). *Annu. Rev. Biochem.* 80:327–332. http://dx.doi.org/10.1146/annurev-biochem-121010-125553

Liu, X., C.A. Thorling, L. Jin, and M.S. Roberts. 2012. Intravital multiphoton imaging of rhodamine 123 in the rat liver after intravenous dosing. *IntraVital*. 1:54–59. http://dx.doi.org/10.4161/intv.21450

Livet, J., T.A. Weissman, H. Kang, R.W. Draft, J. Lu, R.A. Bennis, J.R. Sanes, and J.W. Lichtman. 2007. Transgenic strategies for combinatorial expression of fluorescent proteins in the nervous system. *Nature*. 450:56–62. http://dx.doi.org/10.1038/nature06293

Llewellyn, M.E., R.P. Barretto, S.L. Delp, and M.J. Schnitzer. 2008. Minimally invasive high-speed imaging of sarcomere contractile dynamics in mice and humans. *Nature*. 454:784–788.

Lo Celso, C., H.E. Fleming, J.W. Wu, C.X. Zhao, S. Miake-Lye, J. Fujisaki, D. Côté, D.W. Rowe, C.P. Lin, and D.T. Scadden. 2009. Live-animal tracking of individual haematopoietic stem/progenitor cells in their niche. *Nature*. 457:92–96. http://dx.doi.org/10.1038/nature07434

MacDonald, I.C., E.E. Schmidt, V.L. Morris, A.F. Chambers, and A.C. Groom. 1992. Intravital videomicroscopy of the chorioallantoic microcirculation: a model system for studying metastasis. *Microvasc. Res.* 44:185–199. http://dx.doi.org/10.1016/0026-2862(92)90079-5

Masamoto, K., Y. Tomita, H. Toriumi, I. Aoki, M. Unekawa, H. Takuwa, Y. Itoh, N. Suzuki, and I. Kanno. 2012. Repeated longitudinal in vivo imaging of neuro-glio-vascular unit at the peripheral boundary of ischemia in mouse cerebral cortex. *Neuroscience*. 212:190–200. http://dx.doi.org/10.1016/j.neuroscience.2012.03.034

Masedunskas, A., and R. Weigert. 2008. Intravital two-photon microscopy for studying the uptake and trafficking of fluorescently conjugated molecules in live rodents. *Traffic*. 9:1801–1810. http://dx.doi.org/10.1111/j.1600-0854.2008.00798.x

Masedunskas, A., M. Sramkova, L. Parente, K.U. Sales, P. Amornphimoltham, T.H. Bugge, and R. Weigert. 2011a. Role for the actomyosin complex in regulated exocytosis revealed by intravital microscopy. *Proc. Natl. Acad. Sci. USA*. 108:13552–13557. http://dx.doi.org/10.1073/pnas.1016778108

Masedunskas, A., M. Sramkova, and R. Weigert. 2011b. Homeostasis of the apical plasma membrane during regulated exocytosis in the salivary glands of live rodents. *Bioarchitecture*. 1:225–229. http://dx.doi.org/10.4161/bioa.18405

Masedunskas, A., O. Milberg, N. Porat-Shliom, M. Sramkova, T. Wigand, P. Amornphimoltham, and R. Weigert. 2012a. Intravital microscopy: A practical guide on imaging intracellular structures in live animals. *Bioarchitecture*. 2:143–157. http://dx.doi.org/10.4161/bioa.21758

Masedunskas, A., N. Porat-Shliom, K. Rechache, M.P. Aye, and R. Weigert. 2012b. Intravital microscopy reveals differences in the kinetics of endocytic pathways between cell cultures and live animals. *Cells*. 1:1121–1132. http://dx.doi.org/10.3390/cells1041121

Masedunskas, A., N. Porat-Shliom, and R. Weigert. 2012c. Linking differences in membrane tension with the requirement for a contractile actomyosin scaffold during exocytosis in salivary glands. *Commun. Integr. Biol*. 5:84–87. http://dx.doi.org/10.4161/cib.18258

Masedunskas, A., N. Porat-Shliom, and R. Weigert. 2012d. Regulated exocytosis: novel insights from intravital microscopy. *Traffic*. 13:627–634. http://dx.doi.org/10.1111/j.1600-0854.2012.01328.x

Masedunskas, A., M. Sramkova, L. Parente, and R. Weigert. 2013. Intravital microscopy to image membrane trafficking in live rats. *Methods Mol. Biol.* 931:153–167. http://dx.doi.org/10.1007/978-1-62703-056-4_9

McGavern, D.B., and S.S. Kang. 2011. Illuminating viral infections in the nervous system. *Nat. Rev. Immunol.* 11:318–329. http://dx.doi.org/10.1038/nri2971

Merlini, M., D. Davalos, and K. Akassoglu. 2012. In vivo imaging of the neurovascular unit in CNS disease. *IntraVital*. 1:87–94. http://dx.doi.org/10.4161/intv.22214

Müller, M., and A. Zumbusch. 2007. Coherent anti-Stokes Raman Scattering Microscopy. *ChemPhysChem*. 8:2156–2170. http://dx.doi.org/10.1002/cphc.200700202

Nakano, A. 2002. Spinning-disk confocal microscopy — a cutting-edge tool for imaging of membrane traffic. *Cell Struct. Funct.* 27:349–355. http://dx.doi.org/10.1247/csf.27.349

Nayak, D., B. Zinselmeyer, K. Corps, and D. McGavern. 2012. In vivo dynamics of innate immune sentinels in the CNS. *IntraVital*. 1:95–106. http://dx.doi.org/10.4161/intv.22823

Nitschke, C., A. Garin, M. Kosco-Vilbois, and M. Gunzer. 2008. 3D and 4D imaging of immune cells in vitro and in vivo. *Histochem. Cell Biol.* 130:1053–1062. http://dx.doi.org/10.1007/s00418-008-0520-x

Nitschké, M., D. Aebischer, M. Abadier, S. Haener, M. Lucic, B. Vigl, H. Luche, H.J. Fehling, O. Biehlmaier, R. Lyck, and C. Halin. 2012. Differential requirement for ROCK in dendritic cell migration within lymphatic capillaries in steady-state and inflammation. *Blood*. 120:2249–2258. http://dx.doi.org/10.1182/blood-2012-03-417923

Nuttall, A.L. 1987. Velocity of red blood cell flow in capillaries of the guinea pig cochlea. *Hear. Res.* 27:121–128. http://dx.doi.org/10.1016/0378-5955(87)90013-X

Nyman, L.R., K.S. Wells, W.S. Head, M. McCaughey, E. Ford, M. Brissova, D.W. Piston, and A.C. Powers. 2008. Real-time, multidimensional in vivo imaging used to investigate blood flow in mouse pancreatic islets. *J. Clin. Invest.* 118:3790–3797. http://dx.doi.org/10.1172/JCI36209

O'Rourke, N.A., and S.E. Fraser. 1990. Dynamic changes in optic fiber terminal arbors lead to retinotopic map formation: an in vivo confocal microscopic study. *Neuron*. 5:159–171. http://dx.doi.org/10.1016/0896-6273(90)90306-Z

Oh, P., P. Borgström, H. Witkiewicz, Y. Li, B.J. Borgström, A. Chrastina, K. Iwata, K.R. Zinn, R. Baldwin, J.E. Testa, and J.E. Schnitzer. 2007. Live dynamic imaging of caveolae pumping targeted antibody rapidly and specifically across endothelium in the lung. *Nat. Biotechnol.* 25:327–337. http://dx.doi.org/10.1038/nbt1292

Oheim, M., D.J. Michael, M. Geisbauer, D. Madsen, and R.H. Chow. 2006. Principles of two-photon excitation fluorescence microscopy and other nonlinear imaging approaches. *Adv. Drug Deliv. Rev.* 58:788–808. http://dx.doi.org/10.1016/j.addr.2006.07.005

Orth, J.D., R.H. Kohler, F. Foijer, P.K. Sorger, R. Weissleder, and T.J. Mitchison. 2011. Analysis of mitosis and antimitotic drug responses in tumors by in vivo microscopy and single-cell pharmacodynamics. *Cancer Res.* 71:4608–4616. http://dx.doi.org/10.1158/0008-5472.CAN-11-0412

Pan, F., and W.B. Gan. 2008. Two-photon imaging of dendritic spine development in the mouse cortex. *Dev. Neurobiol.* 68:771–778. http://dx.doi.org/10.1002/dneu.20630

Paxian, M., S.A. Keller, B. Cross, T.T. Huynh, and M.G. Clemens. 2004. High-resolution visualization of oxygen distribution in the liver in vivo. *Am. J. Physiol. Gastrointest. Liver Physiol.* 286:G37–G44. http://dx.doi.org/10.1152/ajpgi.00041.2003

Pinner, S., P. Jordan, K. Sharrock, L. Bazley, L. Collinson, R. Marais, E. Bonvin, C. Goding, and E. Sahai. 2009. Intravital imaging reveals transient changes in pigment production and Brn2 expression during metastatic melanoma dissemination. *Cancer Res.* 69:7969–7977. http://dx.doi.org/10.1158/0008-5472.CAN-09-0781

Pittet, M.J., and R. Weissleder. 2011. Intravital imaging. *Cell*. 147:983–991. http://dx.doi.org/10.1016/j.cell.2011.11.004

Porat-Shliom, N., O. Milberg, A. Masedunskas, and R. Weigert. 2013. Multiple roles for the actin cytoskeleton during regulated exocytosis. *Cell. Mol. Life Sci.* 70:2099–2121. http://dx.doi.org/10.1007/s00018-012-1156-5

Presson, R.G. Jr., M.B. Brown, A.J. Fisher, R.M. Sandoval, K.W. Dunn, K.S. Lorenz, E.J. Delp, P. Salama, B.A. Molitoris, and I. Petrache. 2011. Two-photon imaging within the murine thorax without respiratory and cardiac motion artifact. *Am. J. Pathol.* 179:75–82. http://dx.doi.org/10.1016/j.ajpath.2011.03.048

Provenzano, P.P., K.W. Eliceiri, and P.J. Keely. 2009. Multiphoton microscopy and fluorescence lifetime imaging microscopy (FLIM) to monitor metastasis and the tumor microenvironment. *Clin. Exp. Metastasis*. 26:357–370. http://dx.doi.org/10.1007/s10585-008-9204-0

Qi, H., J.G. Egen, A.Y. Huang, and R.N. Germain. 2006. Extrafollicular activation of lymph node B cells by antigen-bearing dendritic cells. *Science*. 312:1672–1676. http://dx.doi.org/10.1126/science.1125703

Riedl, J., K.C. Flynn, A. Raducanu, F. Gärtner, G. Beck, M. Bösl, F. Bradke, S. Massberg, A. Aszodi, M. Sixt, and R. Wedlich-Söldner. 2010. Lifeact mice for studying F-actin dynamics. *Nat. Methods*. 7:168–169. http://dx.doi.org/10.1038/nmeth0310-168

Ritsma, L., B. Ponsioen, and J. van Rheenen. 2012a. Intravital imaging of cell signaling in mice. *IntraVital*. 1:2–10. http://dx.doi.org/10.4161/intv.20802

Ritsma, L., E.J. Steller, E. Beerling, C.J. Loomans, A. Zomer, C. Gerlach, N. Vrisekoop, D. Seinstra, L. van Gurp, R. Schäfer, et al. 2012b. Intravital microscopy through an abdominal imaging window reveals a pre-micrometastasis stage during liver metastasis. *Sci. Transl. Med.* 4:158ra145. http://dx.doi.org/10.1126/scitranslmed.3004394

Ritsma, L., E.J. Steller, S.I. Ellenbroek, O. Kranenburg, I.H. Borel Rinkes, and J. van Rheenen. 2013. Surgical implantation of an abdominal imaging window for intravital microscopy. *Nat. Protoc.* 8:583–594. http://dx.doi.org/10.1038/nprot.2013.026

Rohde, C.B., and M.F. Yanik. 2011. Subcellular in vivo time-lapse imaging and optical manipulation of *Caenorhabditis elegans* in standard multiwell plates. *Nat Commun*. 2:271. http://dx.doi.org/10.1038/ncomms1266

Rompolas, P., E.R. Deschene, G. Zito, D.G. Gonzalez, I. Saotome, A.M. Haberman, and V. Greco. 2012. Live imaging of stem cell and progeny behaviour in physiological hair-follicle regeneration. *Nature*. 487:496–499. http://dx.doi.org/10.1038/nature11218

Rudolf, R., P.J. Magalhães, and T. Pozzan. 2006. Direct in vivo monitoring of sarcoplasmic reticulum Ca^{2+} and cytosolic cAMP dynamics in mouse skeletal muscle. *J. Cell Biol.* 173:187–193. http://dx.doi.org/10.1083/jcb.200601160

Russo, L.M., R.M. Sandoval, M. McKee, T.M. Osicka, A.B. Collins, D. Brown, B.A. Molitoris, and W.D. Comper. 2007. The normal kidney filters nephrotic levels of albumin retrieved by proximal tubule cells: retrieval is disrupted in nephrotic states. *Kidney Int.* 71:504–513. http://dx.doi.org/10.1038/sj.ki.5002041

Sandoval, R.M., M.D. Kennedy, P.S. Low, and B.A. Molitoris. 2004. Uptake and trafficking of fluorescent conjugates of folic acid in intact kidney determined using intravital two-photon microscopy. *Am. J. Physiol. Cell Physiol.* 287:C517–C526. http://dx.doi.org/10.1152/ajpcell.00006.2004

Smith, B.R., Z. Cheng, A. De, A.L. Koh, R. Sinclair, and S.S. Gambhir. 2008. Real-time intravital imaging of RGD-quantum dot binding to luminal endothelium in mouse tumor neovasculature. *Nano Lett.* 8:2599–2606. http://dx.doi.org/10.1021/nl080141f

Spires, T.L., M. Meyer-Luehmann, E.A. Stern, P.J. McLean, J. Skoch, P.T. Nguyen, B.J. Bacskai, and B.T. Hyman. 2005. Dendritic spine abnormalities

in amyloid precursor protein transgenic mice demonstrated by gene transfer and intravital multiphoton microscopy. *J. Neurosci.* 25:7278–7287. http://dx.doi.org/10.1523/JNEUROSCI.1879-05.2005

Sramkova, M., A. Masedunskas, L. Parente, A. Molinolo, and R. Weigert. 2009. Expression of plasmid DNA in the salivary gland epithelium: novel approaches to study dynamic cellular processes in live animals. *Am. J. Physiol. Cell Physiol.* 297:C1347–C1357. http://dx.doi.org/10.1152/ajpcell.00262.2009

Sramkova, M., A. Masedunskas, and R. Weigert. 2012. Plasmid DNA is internalized from the apical plasma membrane of the salivary gland epithelium in live animals. *Histochem. Cell Biol.* 138:201–213. http://dx.doi.org/10.1007/s00418-012-0959-7

Stockholm, D., M. Bartoli, G. Sillon, N. Bourg, J. Davoust, and I. Richard. 2005. Imaging calpain protease activity by multiphoton FRET in living mice. *J. Mol. Biol.* 346:215–222. http://dx.doi.org/10.1016/j.jmb.2004.11.039

Sun, C.K., X.Y. Zhang, P.W. Sheard, A. Mabuchi, and A.M. Wheatley. 2005. Change in mitochondrial membrane potential is the key mechanism in early warm hepatic ischemia-reperfusion injury. *Microvasc. Res.* 70:102–110. http://dx.doi.org/10.1016/j.mvr.2005.04.003

Svoboda, K., and R. Yasuda. 2006. Principles of two-photon excitation microscopy and its applications to neuroscience. *Neuron*. 50:823–839. http://dx.doi.org/10.1016/j.neuron.2006.05.019

Theer, P., and W. Denk. 2006. On the fundamental imaging-depth limit in two-photon microscopy. *J. Opt. Soc. Am. A Opt. Image Sci. Vis.* 23:3139–3149. http://dx.doi.org/10.1364/JOSAA.23.003139

Theer, P., M.T. Hasan, and W. Denk. 2003. Two-photon imaging to a depth of 1000 microm in living brains by use of a Ti:Al2O3 regenerative amplifier. *Opt. Lett.* 28:1022–1024. http://dx.doi.org/10.1364/OL.28.001022

Theruvath, T.P., M.C. Snoddy, Z. Zhong, and J.J. Lemasters. 2008. Mitochondrial permeability transition in liver ischemia and reperfusion: role of c-Jun N-terminal kinase 2. *Transplantation*. 85:1500–1504. http://dx.doi.org/10.1097/TP.0b013e31816fefb5

Thomsen, P., K. Roepstorff, M. Stahlhut, and B. van Deurs. 2002. Caveolae are highly immobile plasma membrane microdomains, which are not involved in constitutive endocytic trafficking. *Mol. Biol. Cell*. 13:238–250. http://dx.doi.org/10.1091/mbc.01-06-0317

Thorogood, P., and A. Wood. 1987. Analysis of in vivo cell movement using transparent tissue systems. *J. Cell Sci. Suppl.* 8:395–413. http://dx.doi.org/10.1242/jcs.1987.Supplement_8.22

Tozer, G.M., S.M. Ameer-Beg, J. Baker, P.R. Barber, S.A. Hill, R.J. Hodgkiss, R. Locke, V.E. Prise, I. Wilson, and B. Vojnovic. 2005. Intravital imaging of tumour vascular networks using multi-photon fluorescence microscopy. *Adv. Drug Deliv. Rev.* 57:135–152. http://dx.doi.org/10.1016/j.addr.2004.07.015

Tserevelakis, G.J., G. Filippidis, E.V. Megalou, C. Fotakis, and N. Tavernarakis. 2011. Cell tracking in live *Caenorhabditis elegans* embryos via third harmonic generation imaging microscopy measurements. *J. Biomed. Opt.* 16:046019. http://dx.doi.org/10.1117/1.3569615

Unni, V.K., T.A. Weissman, E. Rockenstein, E. Masliah, P.J. McLean, and B.T. Hyman. 2010. In vivo imaging of alpha-synuclein in mouse cortex demonstrates stable expression and differential subcellular compartment mobility. *PLoS ONE*. 5:e10589. http://dx.doi.org/10.1371/journal.pone.0010589

Vakoc, B.J., R.M. Lanning, J.A. Tyrrell, T.P. Padera, L.A. Bartlett, T. Stylianopoulos, L.L. Munn, G.J. Tearney, D. Fukumura, R.K. Jain, and B.E. Bouma. 2009. Three-dimensional microscopy of the tumor microenvironment in vivo using optical frequency domain imaging. *Nat. Med.* 15:1219–1223. http://dx.doi.org/10.1038/nm.1971

Villringer, A., R.L. Haberl, U. Dirnagl, F. Anneser, M. Verst, and K.M. Einhäupl. 1989. Confocal laser microscopy to study microcirculation on the rat brain surface in vivo. *Brain Res.* 504:159–160. http://dx.doi.org/10.1016/0006-8993(89)91616-8

von Andrian, U.H. 1996. Intravital microscopy of the peripheral lymph node microcirculation in mice. *Microcirculation*. 3:287–300. http://dx.doi.org/10.3109/10739689609148303

Wagner, R. 1839. Erlauterungstaflen zur Physiologie und Entwicklungsgeschichte. Leopold Voss, Leipzig, Germany.

Wang, W., J.B. Wyckoff, S. Goswami, Y. Wang, M. Sidani, J.E. Segall, and J.S. Condeelis. 2007. Coordinated regulation of pathways for enhanced cell motility and chemotaxis is conserved in rat and mouse mammary tumors. *Cancer Res.* 67:3505–3511. http://dx.doi.org/10.1158/0008-5472.CAN-06-3714

Weigelin, B., G.-J. Bakker, and P. Friedl. 2012. Intravital third harmonic generation microscopy of collective melanoma cell invasion: Principles of interface guidance and microvesicle dynamics. *IntraVital*. 1:32–43. http://dx.doi.org/10.4161/intv.21223

Weigert, R., M. Sramkova, L. Parente, P. Amornphimoltham, and A. Masedunskas. 2010. Intravital microscopy: a novel tool to study cell biology in living animals. *Histochem. Cell Biol.* 133:481–491. http://dx.doi.org/10.1007/s00418-010-0692-z

Wilson, T. 2002. Confocal microscopy: Basic principles and architectures. *In* Confocal and Two-Photon Microscopy: Foundations, Applications and Advances. Alberto Diaspro, editor. Wiley-Liss, Inc., New York. 19–38 pp.

Wood, A., and P. Thorogood. 1984. An analysis of in vivo cell migration during teleost fin morphogenesis. *J. Cell Sci.* 66:205–222.

Wyckoff, J.B., Y. Wang, E.Y. Lin, J.F. Li, S. Goswami, E.R. Stanley, J.E. Segall, J.W. Pollard, and J. Condeelis. 2007. Direct visualization of macrophage-assisted tumor cell intravasation in mammary tumors. *Cancer Res.* 67:2649–2656. http://dx.doi.org/10.1158/0008-5472.CAN-06-1823

Xu, H.T., F. Pan, G. Yang, and W.B. Gan. 2007. Choice of cranial window type for in vivo imaging affects dendritic spine turnover in the cortex. *Nat. Neurosci.* 10:549–551. http://dx.doi.org/10.1038/nn1883

Yu, W., R.M. Sandoval, and B.A. Molitoris. 2007. Rapid determination of renal filtration function using an optical ratiometric imaging approach. *Am. J. Physiol. Renal Physiol.* 292:F1873–F1880. http://dx.doi.org/10.1152/ajprenal.00218.2006

Zariwala, H.A., B.G. Borghuis, T.M. Hoogland, L. Madisen, L. Tian, C.I. De Zeeuw, H. Zeng, L.L. Looger, K. Svoboda, and T.W. Chen. 2012. A Cre-dependent GCaMP3 reporter mouse for neuronal imaging in vivo. *J. Neurosci.* 32:3131–3141. http://dx.doi.org/10.1523/JNEUROSCI.4469-11.2012

Zhang, S., and T.H. Murphy. 2007. Imaging the impact of cortical microcirculation on synaptic structure and sensory-evoked hemodynamic responses in vivo. *PLoS Biol.* 5:e119. http://dx.doi.org/10.1371/journal.pbio.0050119

Zhong, Z., V.K. Ramshesh, H. Rehman, R.T. Currin, V. Sridharan, T.P. Theruvath, I. Kim, G.L. Wright, and J.J. Lemasters. 2008. Activation of the oxygen-sensing signal cascade prevents mitochondrial injury after mouse liver ischemia-reperfusion. *Am. J. Physiol. Gastrointest. Liver Physiol.* 295:G823–G832. http://dx.doi.org/10.1152/ajpgi.90287.2008

Zipfel, W.R., R.M. Williams, R. Christie, A.Y. Nikitin, B.T. Hyman, and W.W. Webb. 2003a. Live tissue intrinsic emission microscopy using multiphoton-excited native fluorescence and second harmonic generation. *Proc. Natl. Acad. Sci. USA*. 100:7075–7080. http://dx.doi.org/10.1073/pnas.0832308100

Zipfel, W.R., R.M. Williams, and W.W. Webb. 2003b. Nonlinear magic: multiphoton microscopy in the biosciences. *Nat. Biotechnol.* 21:1369–1377. http://dx.doi.org/10.1038/nbt899

Zweifach, B.W. 1954. Direct observation of the mesenteric circulation in experimental animals. *Anat. Rec.* 120:277–291. http://dx.doi.org/10.1002/ar.1091200115